Electronic Supplementary Material (ESI) for RSC Advances.

Supporting Information for:

Direct Electron Transfer from Alcohol Dehydrogenase

Fabio Lima and Gilberto Maia*

Institute of Chemistry, Universidade Federal de Mato Grosso do Sul, Av. Senador Filinto Muller, 1555, Campo Grande, MS 79074-460, Brazil

*To whom correspondence should be addressed

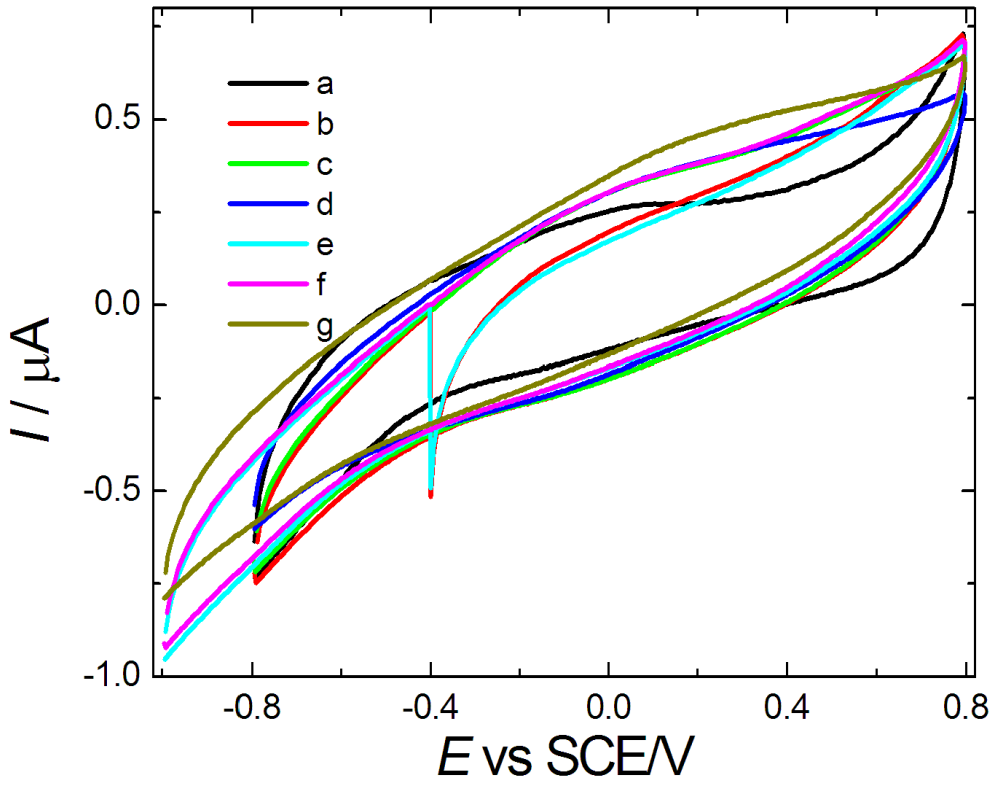

Figure S1. Hydrodynamic cyclic voltammograms for bare GC (*a*, second scan), GC/NAD^+/Nafion (*b*, first; *c*, second; *d*, 30th scan), and GC/NADH/Nafion (*e*, first; *f*, second; *g*, 30th scan) electrodes in N_2-saturated 0.1 M KH_2PO_4 (pH 6.5). First scans started at –0.4 V in the positive-going direction. ω = 200 rpm, ν = 10 mV s^{-1}.

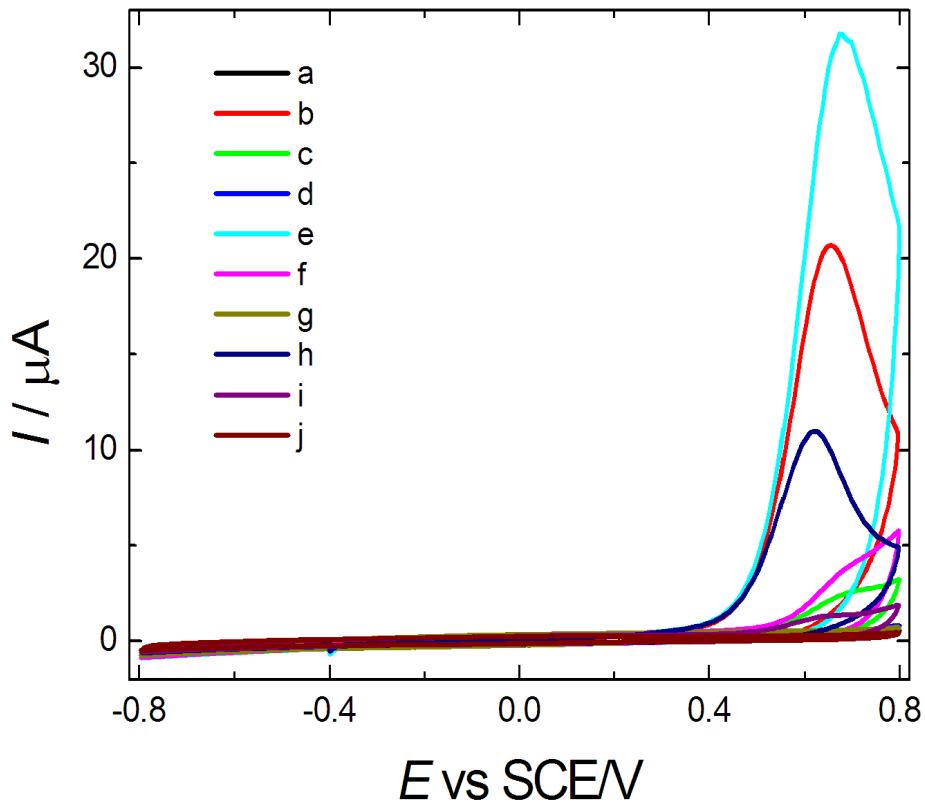

Figure S2. Hydrodynamic cyclic voltammograms for bare GC (*a*, second scan), GC/ADH-NAD^+/Nafion (*b*, first; *c*, second; *d*, 30th scan), GC/ADH-NADH/Nafion (*e*, first; *f*, second; *g*, 30th scan), and GC/PM-ADH-NAD^+/Nafion (*h*, first; *i*, second; *j*, 30th scan) electrodes in N_2-saturated 0.1 M KH_2PO_4 (pH 6.5). First scans started at –0.4 V in the positive-going direction. ω = 200 rpm, ν = 10 mV s^{-1}.

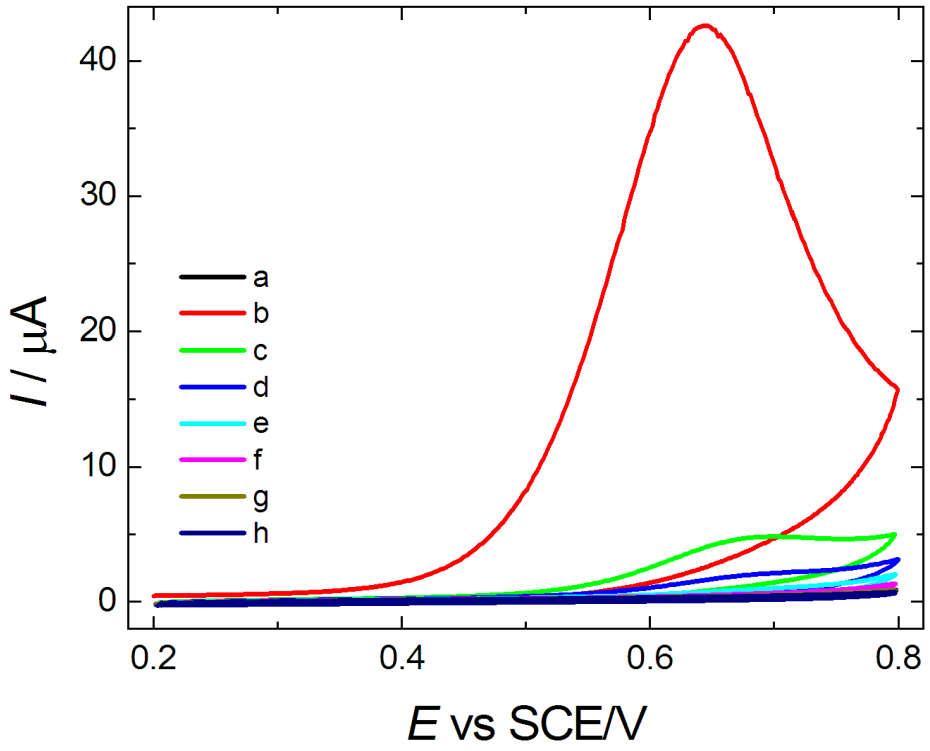

Figure S3. Hydrodynamic cyclic voltammograms for bare GC (*a*, first scan) and GC/ADH-NAD^+/Nafion (*b*, first; *c*, second; *d*, third; *e*, fifth; *f*, 10th; *g*, 20th; *h*, 30th scan) electrodes in N_2-saturated 0.1 M KH_2PO_4 (pH 6.5). First scans started at 0.2 V. ω = 200 rpm, ν = 10 mV s^{-1}.

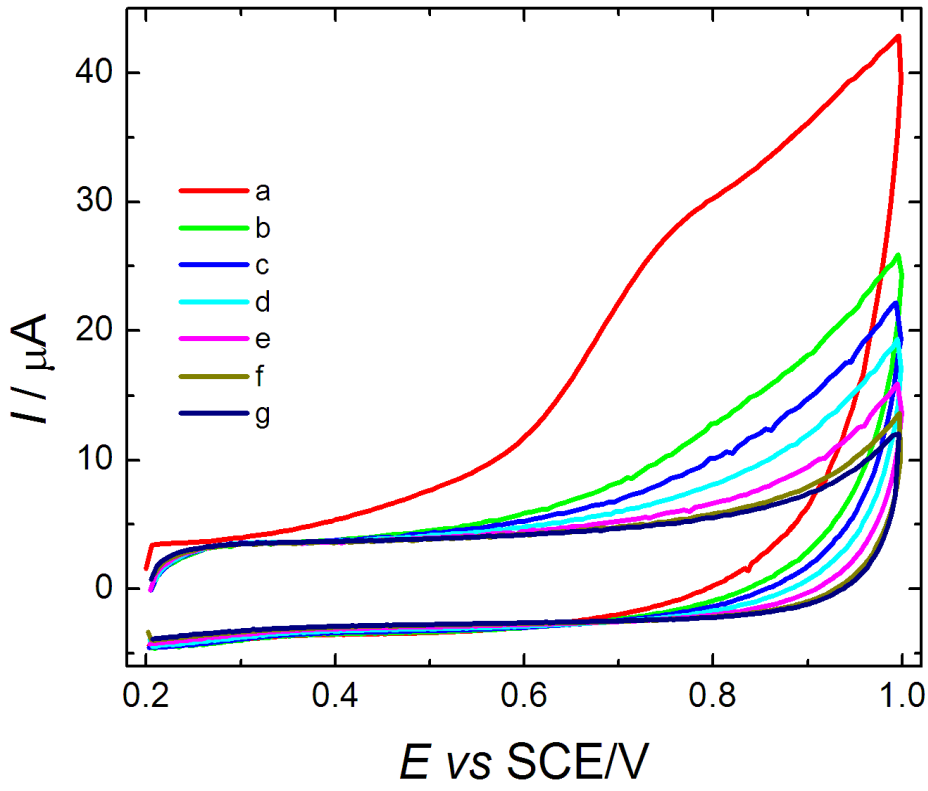

Figure S4. Hydrodynamic cyclic voltammograms for a GC/VC XC-72/PM-ADH/Nafion electrode (*a*, first; *b*, second; *c*, third; *d*, fifth; *e*, 10th; *f*, 20th; *g*, 20th scan) in N_2-saturated 0.1 M KH_2PO_4 (pH 6.5). First scan started at 0.2 V. ω = 200 rpm, ν = 10 mV s^{-1}.

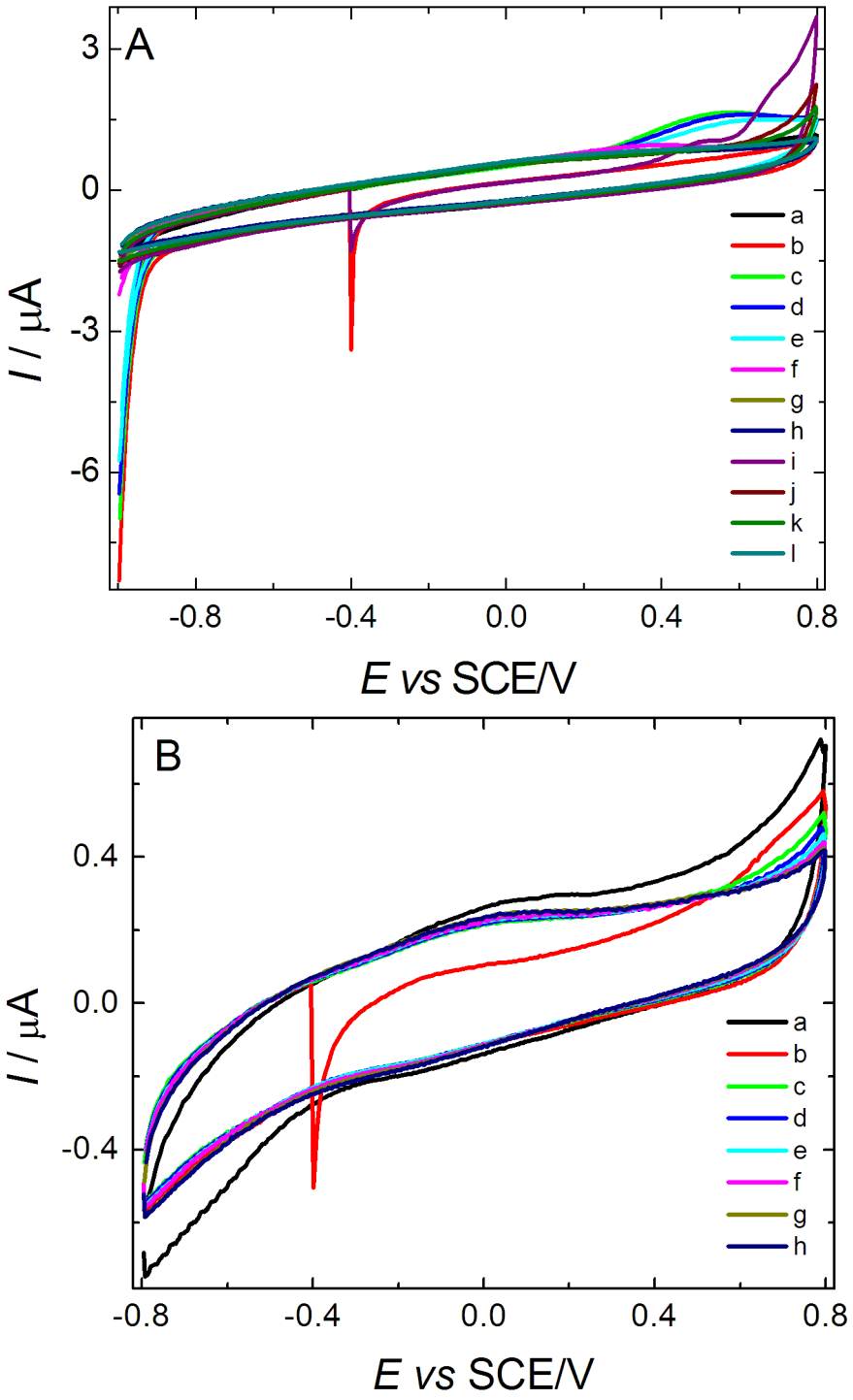

Figure S5. Hydrodynamic cyclic voltammograms for (A) bare GC (*a*, second scan), GC/NAD$^+$/Nafion (*b*, first; *c*, second; *d*, third; *e*, fifth; *f*, 10th; *g*, 20th; *h*, 30th scan), and GC/NADH/Nafion (*i*, first; *j*, second; *k*, third; *l*, 30th scan), and (B) bare GC (*a*, second scan) and (B) GC/NAD$^+$/Nafion (*b*, first; *c*, second; *d*, third; *e*, fifth; *f*, 10th; *g*, 20th; *h*, 30th scan) electrodes in N_2-saturated 0.1 M KH_2PO_4 (pH 6.5) containing 100 mM ethanol. First scans started at –0.4 V in the positive-going direction. ω = 200 rpm, ν = 10 mV s^{-1}.

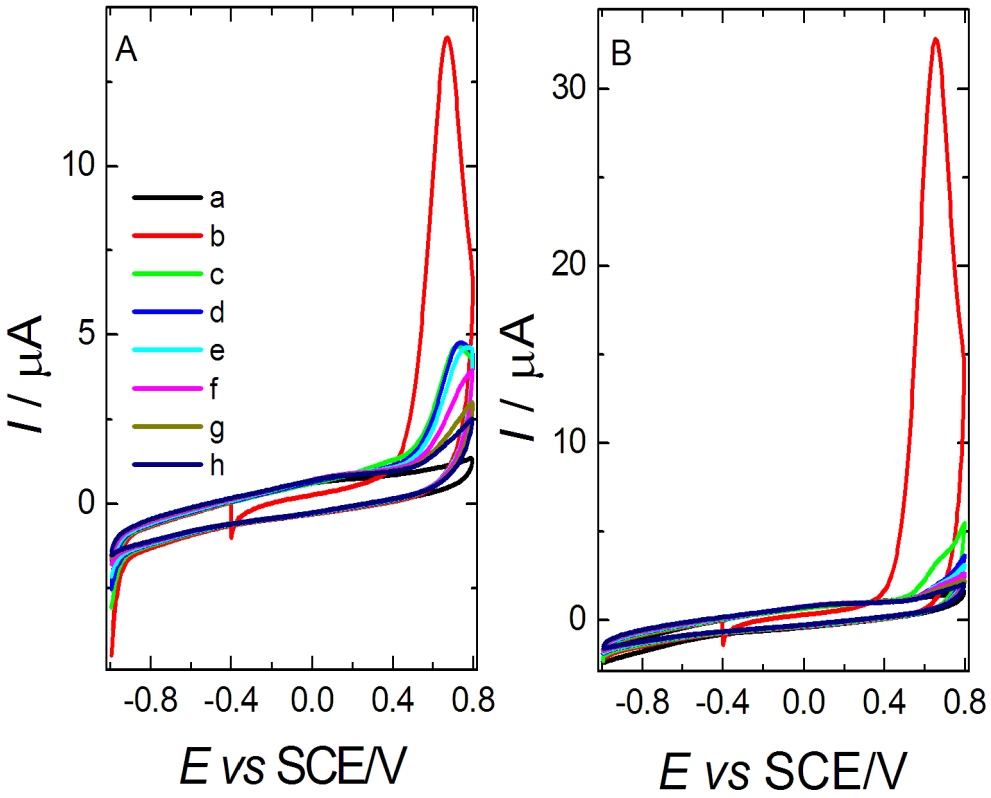

Figure S6. Hydrodynamic cyclic voltammograms for bare GC (*a*, second scan) and for the first (*b*), second (*c*), third (*d*), fifth (*e*), 10th (*f*), 20th (*g*), and 30th (*h*) scans employing (A) GC/ADH-NAD^+/Nafion and (B) GC/ADH-NADH/Nafion electrodes in N_2-saturated 0.1 M KH_2PO_4 (pH 6.5) containing 100 mM ethanol. First scans started at –0.4 V in the positive-going direction. ω = 200 rpm, ν = 10 mV s^{-1}.

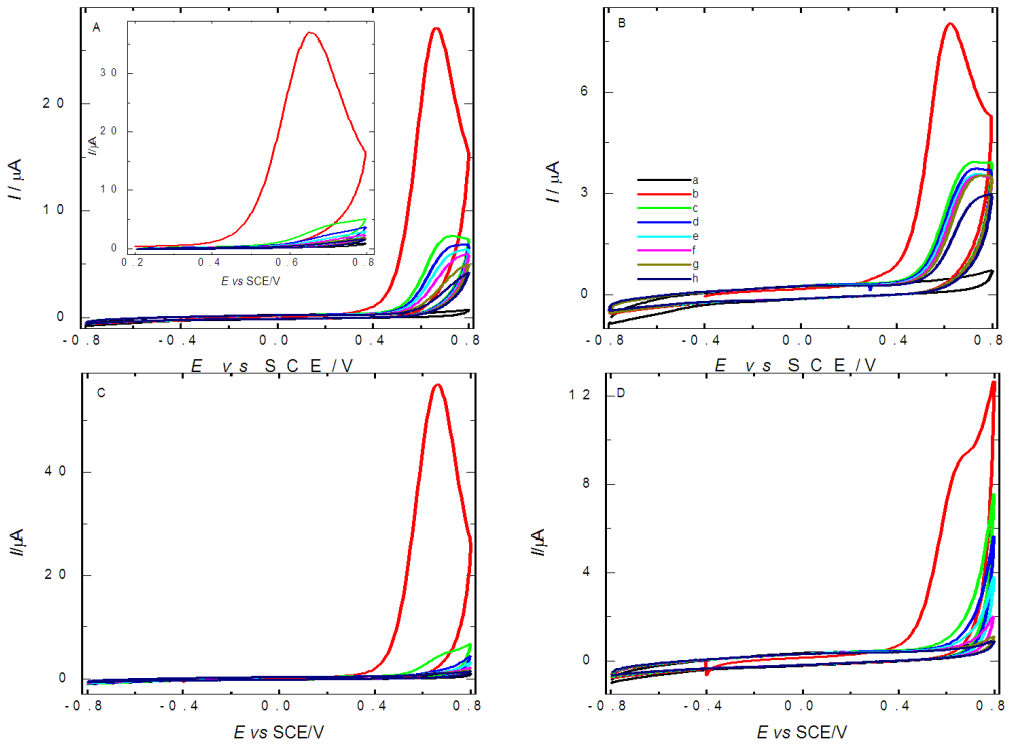

Figure S7. Hydrodynamic cyclic voltammograms for bare GC (*a*, second scan) and for the first (*b*), second (*c*), third (*d*), fifth (*e*), 10th (*f*), 20th (*g*), and 30th (*h*) scans employing (A) GC/ADH-NAD^+/Nafion, (B) GC/PM-ADH-NAD^+/Nafion, (C) GC/ADH-NADH/Nafion, and (D) GC/PM-ADH-NADH/Nafion electrodes in N_2-saturated 0.1 M KH_2PO_4 (pH 6.5) containing 100 mM ethanol. First scans started at –0.4 V in the positive-going direction. ω = 200 rpm, ν = 10 mV s^{-1}. Inset (A): GC/ADH-NAD^+/Nafion, with first scan starting at 0.2 V in the positive-going direction.

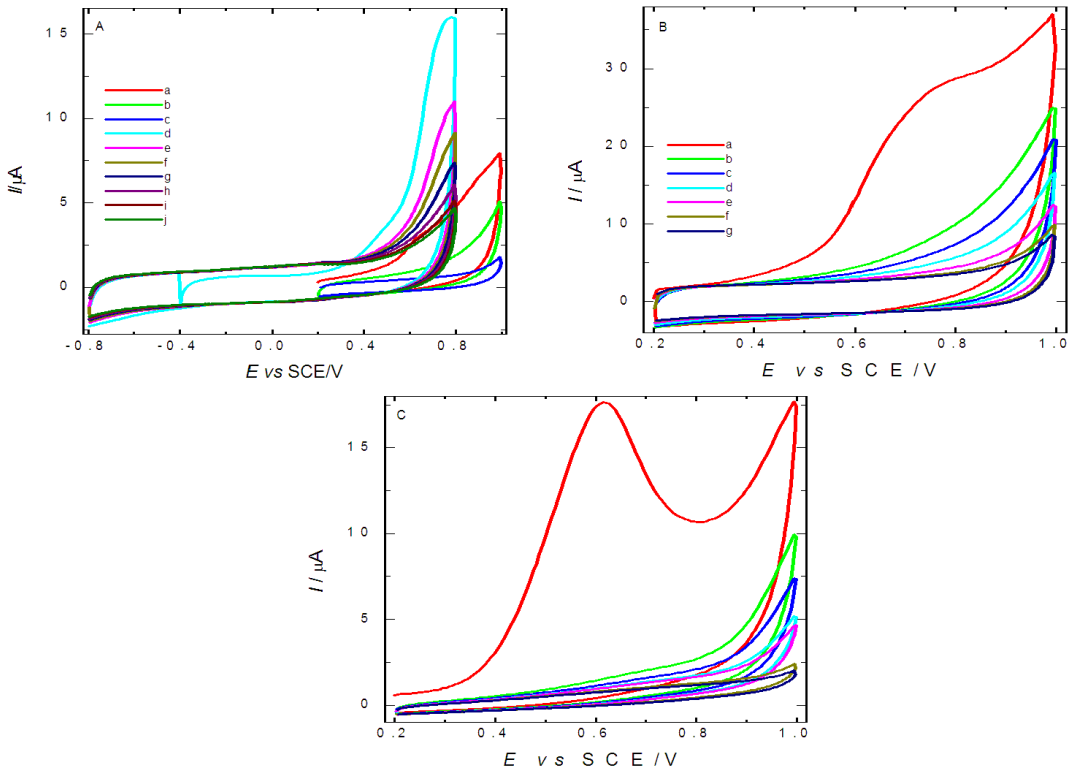

Figure S8. Hydrodynamic cyclic voltammograms for (A) GC/VC XC-72/PM/Nafion (*a*, first; *b*, second; *c*, 30th scan) and GC/VC XC-72/PM-ADH/Nafion (*d*, first; *e*, second; *f*, third; *g*, fifth; *h*, 10th; *i*, 20th; *j*, 30th scan) electrodes, with first scans starting at 0.2 and –0.4 V in the positive-going direction, respectively. Also depicted are the hydrodynamic cyclic voltammograms for the first (*a*), second (*b*), third (*c*), fifth (*d*), 10th (*e*), 20th (*f*), and 30th (*g*) scans employing GC/VC XC-72/PM-ADH/Nafion (B) and GC/VC XC-72/PM-ADH-NAD^+/Nafion (C) electrodes, with scans starting at 0.2 V in the positive-going direction in N_2-saturated 0.1 M KH_2PO_4 (pH 6.5) containing 100 mM ethanol. ω = 200 rpm, ν = 10 mV s^{-1}.

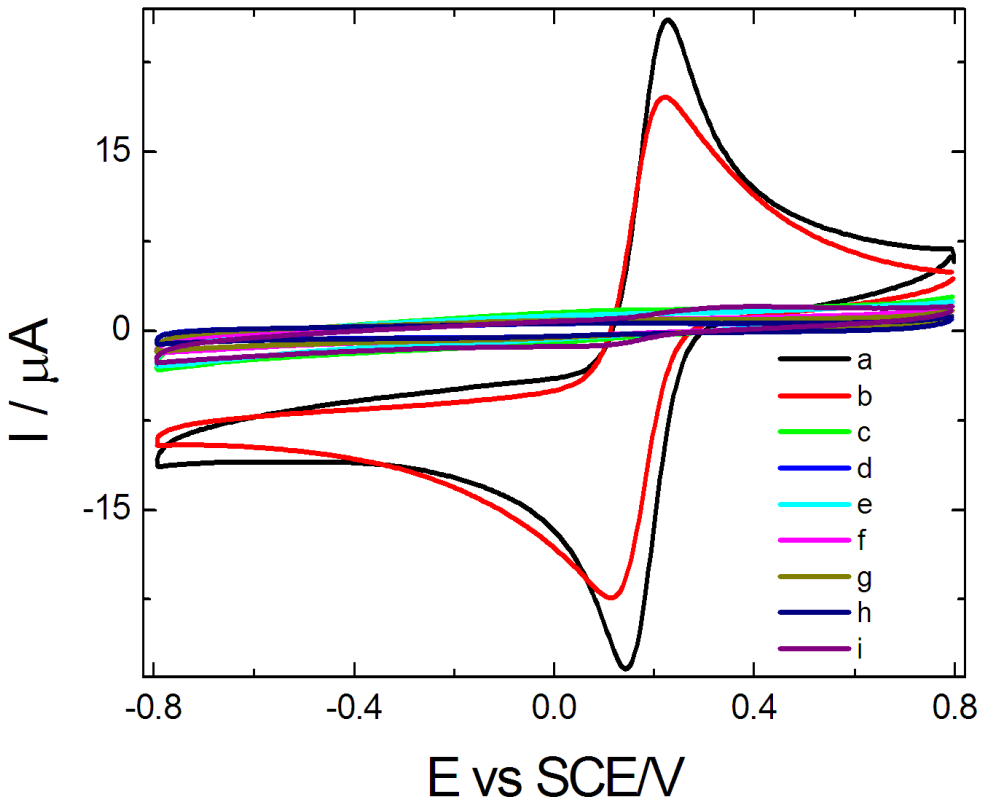

Figure S9. Cyclic voltammograms for bare GC (*a*) and, after 30 HCV scans in 0.1 M KH_2PO_4 (pH 6.5) containing 100 mM ethanol, for bare GC (*b*), GC/ADH/Nafion(in the absence of ethanol) (*c*), GC/PM-ADH/Nafion(in the absence of ethanol) (*d*), GC/NAD^+/Nafion (in the absence of ethanol) (*e*), GC/PM-ADH-NAD^+/Nafion (in the absence of ethanol) (*f*), GC/ADH/Nafion (*g*), GC/PM-ADH/Nafion (*h*), and GC/PM-ADH-NAD^+/Nafion (*i*) electrodes in N_2-saturated 0.1 M KH_2PO_4 (pH 6.5) containing 1 mM $K_3Fe(CN)_6$. ν = 50 mV s^{-1}.

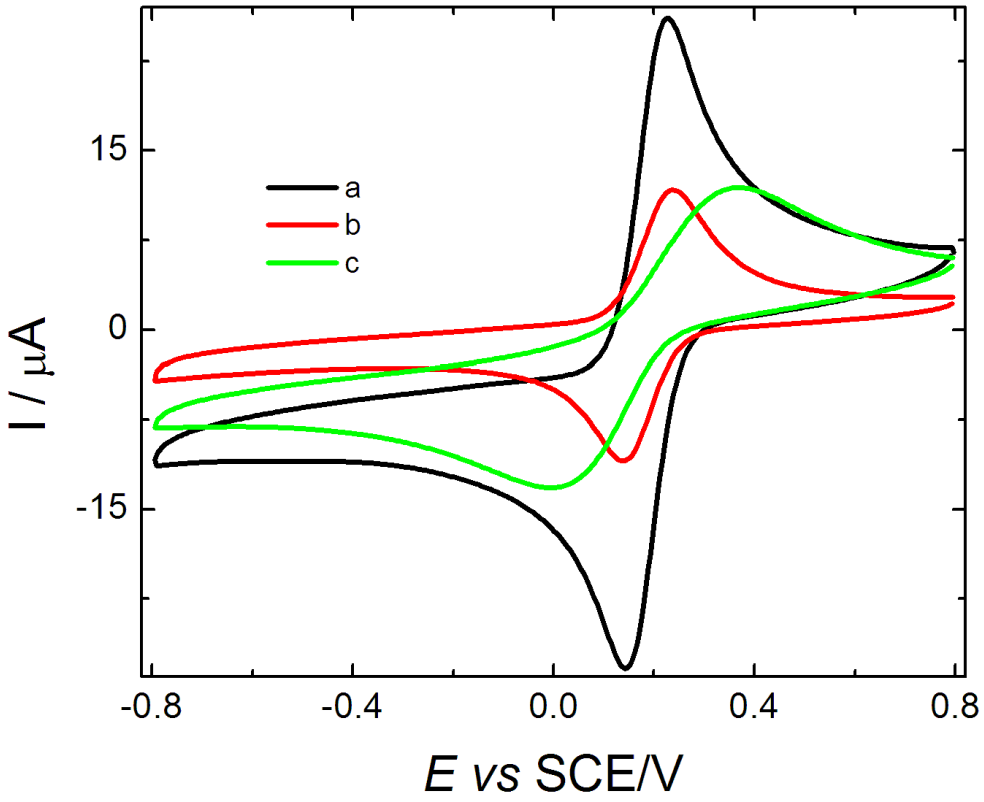

Figure S10. Cyclic voltammograms for bare GC (*a*) and, after 30 HCV scans in 0.1 M KH_2PO_4 (pH 6.5), for GC/NAD^+/Nafion (*b*), and GC/NADH/Nafion (*c*) electrodes in N_2-saturated 0.1 M KH_2PO_4 (pH 6.5) containing 1 m$MK_3Fe(CN)_6$. ν = 50 mV s^{-1}.

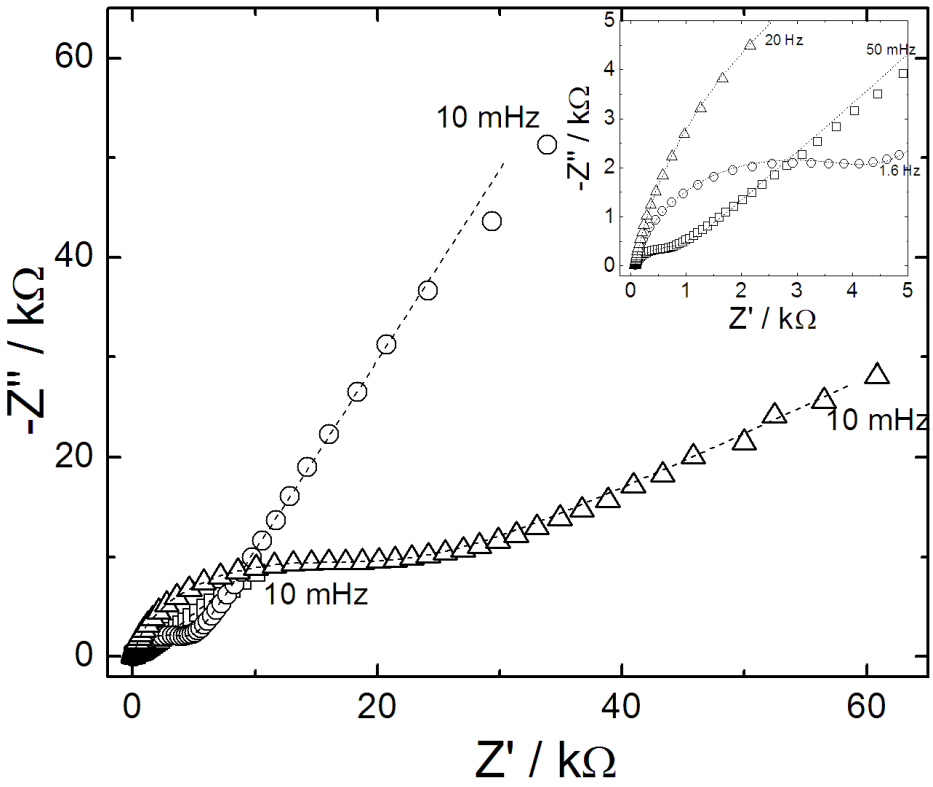

Figure S11. Impedance plane plots for bare GC (●) and, after 30 HCV scans in 0.1 M KH_2PO_4 (pH 6.5), for GC/NAD^+/Nafion (ᔓ), and GC/NADH/Nafion (❒) electrodes in N_2-saturated 0.1 M KH_2PO_4 (pH 6.5) containing 1 m$MK_3Fe(CN)_6$. Potential perturbation: 25 mV (rms). Frequency range: 100 kHz–10 mHz. Constant potential for EIS acquisition: OCP (0.20 V *vs*. SCE on average). Lines represent spectra (adjusted) calculated using a non-linear least-squares program, conforming to the equivalent circuit $R_s[Q_{dl}(R_{ct}W_{lf})]$, or $R_s[Q_{dl}(R_{ct}Q_{lf})]$. Calculated average values: R_s = 77 Ω, Q_{dl} = 3.5 μF s^{n-1}, n = 0.9, and W_{lf} = 56 μF. Inset: Impedance plane plots from the main graph restricted to 5 kΩ.

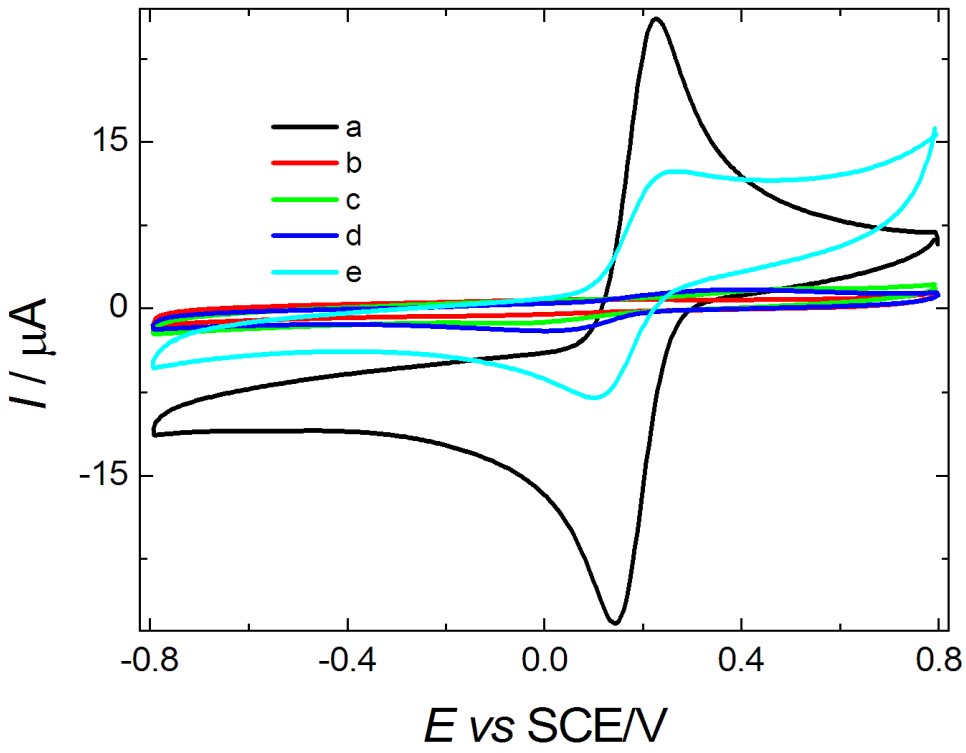

Figure S12. Cyclic voltammograms for bare GC (*a*) and, after 30 HCV scans in 0.1 M KH_2PO_4 (pH 6.5), for GC/ADH-NAD^+/Nafion (*b*), GC/ADH-NADH/Nafion (*c*), GC/PM-ADH-NAD^+/Nafion (*d*), and GC/VC XC-72/PM-ADH/Nafion (*e*) electrodes in N_2-saturated 0.1 M KH_2PO_4 (pH 6.5) containing 1 mM $K_3Fe(CN)_6$. ν = 50 mV s^{-1}.

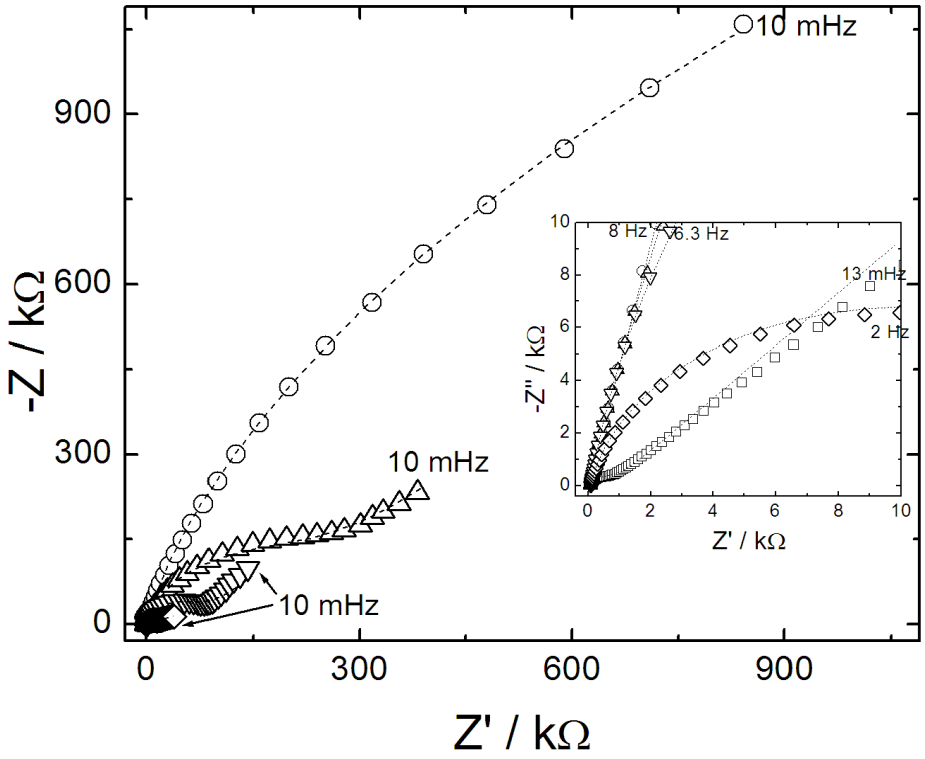

Figure S13. Impedance plane plots for bare GC (⭘) and, after 30 HCV scans in 0.1 M KH_2PO_4 (pH 6.5), for GC/ADH-NAD^+/Nafion (ᘓ), GC/ADH-NADH/Nafion (❒), GC/PM-ADH-NAD^+/Nafion (♦), and GC/VC XC-72/PM-ADH/Nafion (❋) electrodes in N_2-saturated 0.1 M KH_2PO_4 (pH 6.5) containing 1 m$MK_3Fe(CN)_6$. Potential perturbation: 25 mV (rms). Frequency range: 100 kHz–10 mHz. Constant potential for EIS acquisition: OCP (0.14 V *vs*. SCE on average). Lines represent spectra (adjusted) calculated using a non-linear least-squares program, conforming to the equivalent circuit $R_s[Q_{dl}(R_{ct}W_{lf})]$, or $R_s[Q_{dl}(R_{ct}Q_{lf})]$. Calculated average values: R_s = 77 Ω, Q_{dl} = 5.3 μF s^{n-1}, n = 0.9, and W_{lf} = 86 μF. Inset: Impedance plane plots from the main graph restricted to 10 kΩ.

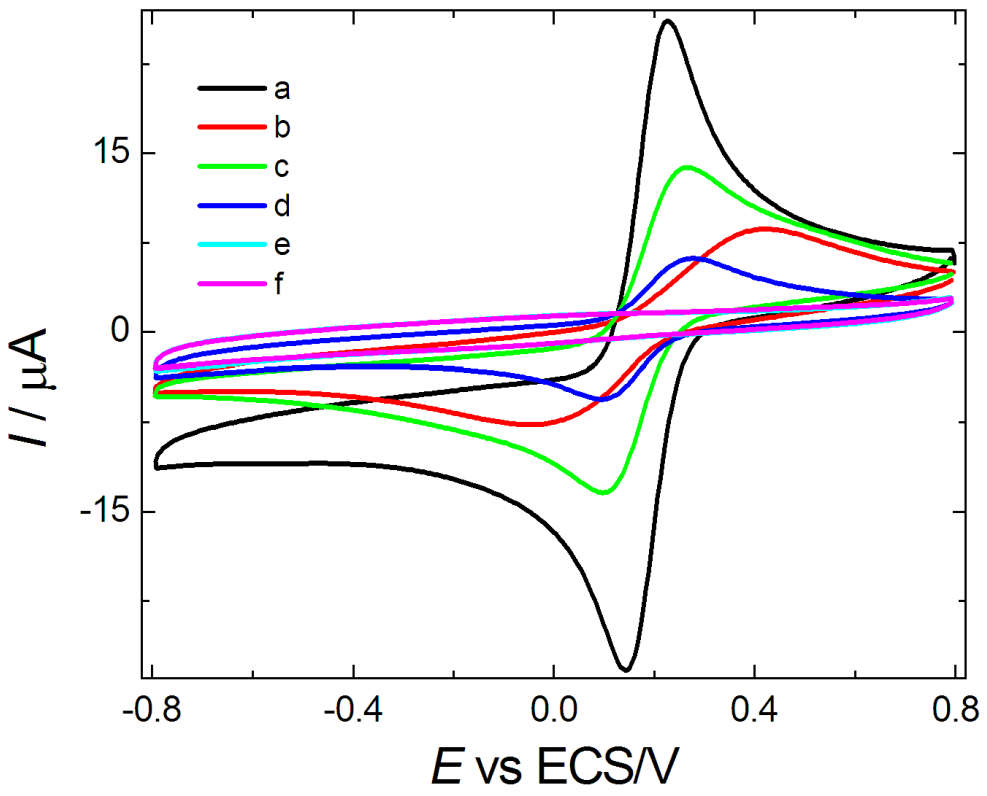

Figure S14. Cyclic voltammograms for bare GC (*a*) and, after 30 HCV scans in 0.1 M KH_2PO_4 (pH 6.5) containing 100 mM ethanol, for GC/NAD^+/Nafion (*b*), GC/NAD^+/Nafion' (*c*), GC/NADH/Nafion (*d*), GC/ADH-NAD^+/Nafion (*e*), and GC/ADH-NADH/Nafion (*f*) electrodes in N_2-saturated 0.1 M KH_2PO_4 (pH 6.5) containing 1 mM $K_3Fe(CN)_6$. ν = 50 mV s^{-1}.

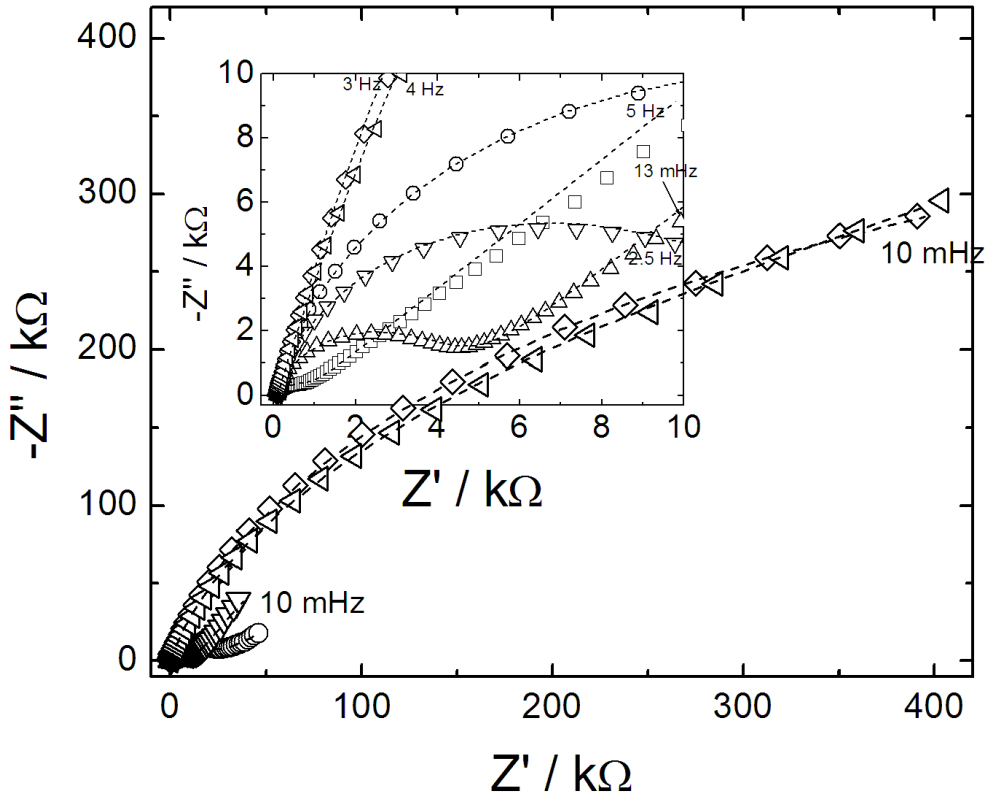

Figure S15. Impedance plane plots for bare GC (⭘) and, after 30 HCV scans in 0.1 M KH_2PO_4 (pH 6.5) containing 100 mM ethanol, for GC/NAD^+/Nafion (ᘓ), GC/NAD^+/Nafion' (❒), GC/NADH/Nafion (♦), GC/ADH-NAD^+/Nafion (❋), and GC/ADH-NADH/Nafion (❖) electrodes in N_2-saturated 0.1 M KH_2PO_4 (pH 6.5) containing 1 m$MK_3Fe(CN)_6$. Potential perturbation: 25 mV (rms). Frequency range: 100 kHz–10 mHz. Constant potential for EIS acquisition: OCP (0.14 V *vs*. SCE on average). Lines represent spectra (adjusted) calculated using a non-linear least-squares program, conforming to the equivalent circuit $R_s[Q_{dl}(R_{ct}W_{lf})]$, or $R_s[Q_{dl}(R_{ct}Q_{lf})]$. Calculated average values: R_s = 83 Ω, Q_{dl} = 6.0 μF s^{n-1}, n = 0.9, and W_{lf} = 104 μF. Inset: Impedance plane plots from the main graph restricted to 10 kΩ.

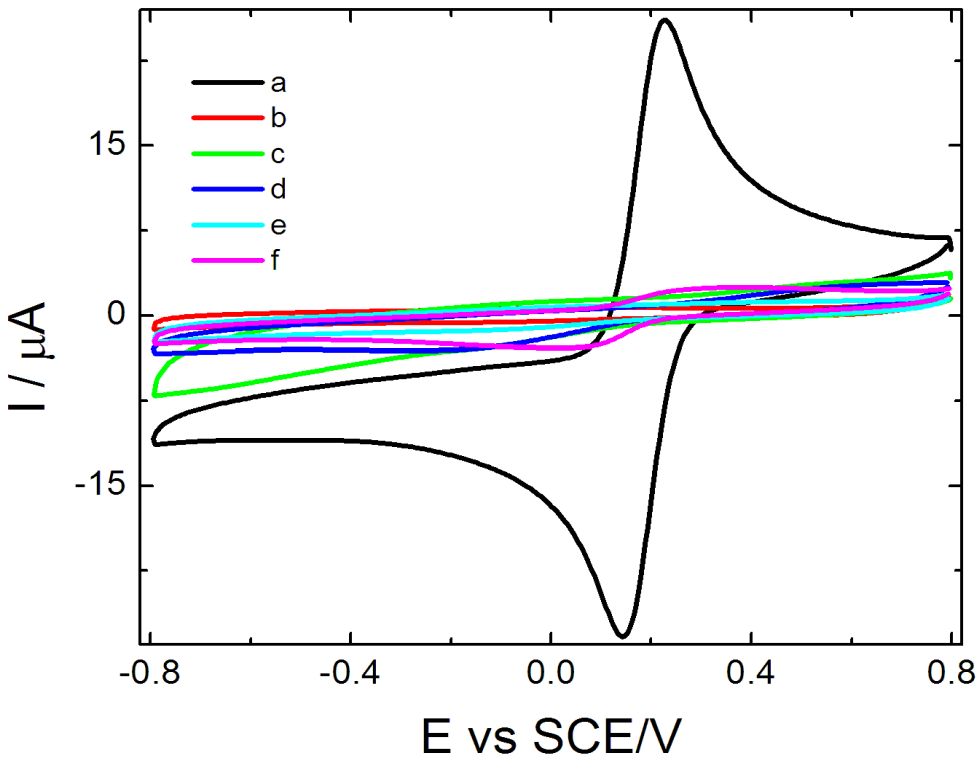

Figure S16. Cyclic voltammograms for bare GC (*a*) and, after 30 HCV scans in 0.1 M KH_2PO_4 (pH 6.5) containing 100 mM ethanol, for GC/ADH-NAD^+/Nafion (*b*), GC/ADH-NAD^+/Nafion (narrow potential scan window) (*c*), GC/PM-ADH-NAD^+/Nafion (*d*), GC/ADH-NADH/Nafion (*e*), and GC/PM-ADH-NADH/Nafion (*f*) electrodes in N_2-saturated 0.1 M KH_2PO_4 (pH 6.5) containing 1 mM $K_3Fe(CN)_6$. ν = 50 mV s^{-1}.

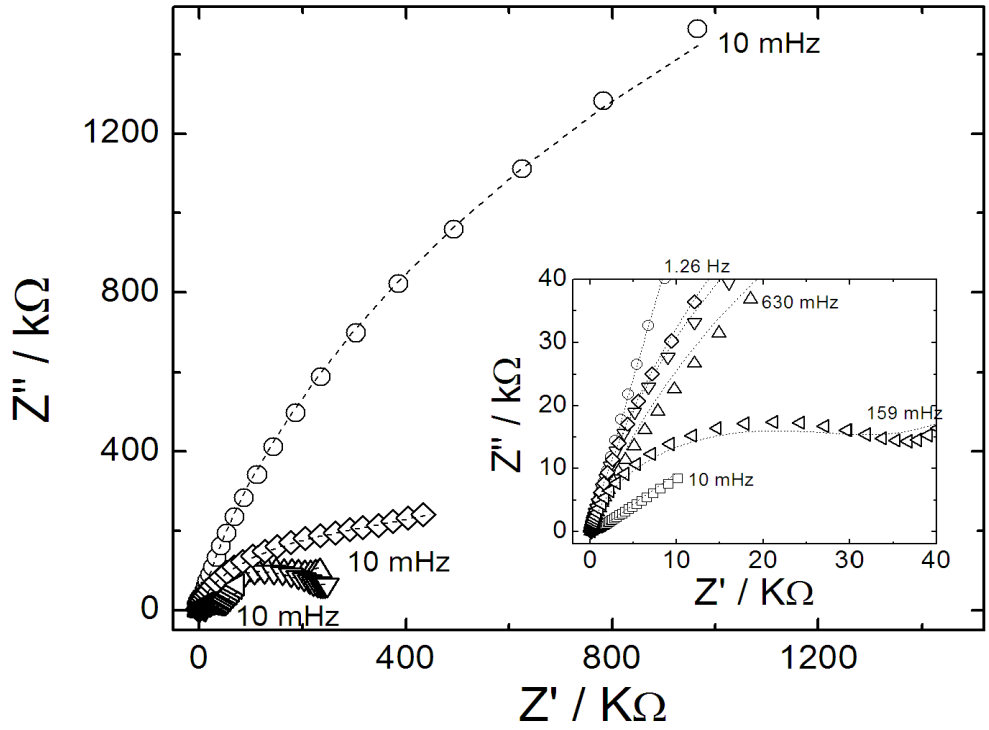

Figure S17. Impedance plane plots for bare GC (⭘) and, after 30 HCV scans in 0.1 M KH_2PO_4 (pH 6.5) containing 100 mM ethanol, for GC/ADH-NAD^+/Nafion (ᘓ), GC/ADH-NAD^+/Nafion (narrow potential scan window) (❒), GC/PM-ADH-NAD^+/Nafion (♦), GC/ADH-NADH/Nafion (❋), and GC/PM-ADH-NADH/Nafion (❖) electrodes in N_2-saturated 0.1 M KH_2PO_4 (pH 6.5) containing 1 mM $K_3Fe(CN)_6$. Potential perturbation: 25 mV (rms). Frequency range: 100 kHz–10 mHz. Constant potential for EIS acquisition: OCP (0.16 V *vs*. SCE on average). Lines represent spectra (adjusted) calculated using a non-linear least-squares program, conforming to the equivalent circuit $R_s[Q_{dl}(R_{ct}W_{lf})]$, or $R_s[Q_{dl}(R_{ct}Q_{lf})]$. Calculated average values: R_s = 87 Ω, Q_{dl} = 6.0 μF s^{n-1}, n = 0.9, and W_{lf} = 76 μF. Inset: Impedance plane plots from the main graph restricted to 40 kΩ.

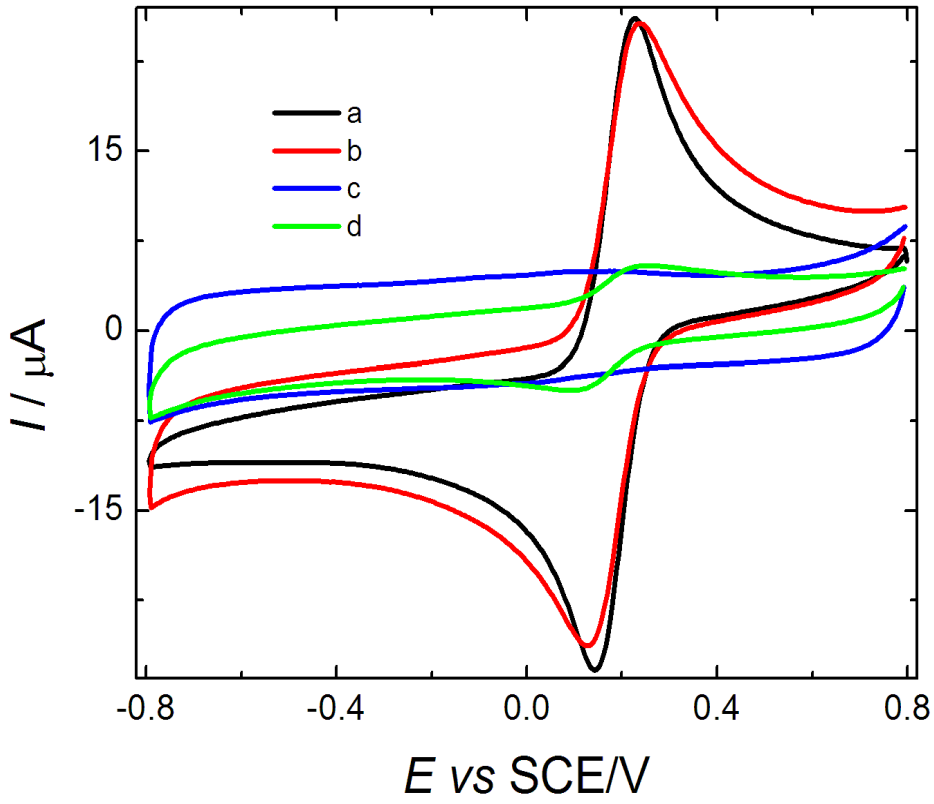

Figure S18. Cyclic voltammograms for bare GC (*a*) and, after 30 HCV scans in 0.1 M KH_2PO_4 (pH 6.5) containing 100 mM ethanol, for GC/VC XC-72/PM/Nafion (*b*), GC/VC XC-72/PM-ADH/Nafion (*c*), and GC/VC XC-72/PM-ADH-NAD^+/Nafion (*d*) electrodes in N_2-saturated 0.1 M KH_2PO_4 (pH 6.5) containing 1 mM $K_3Fe(CN)_6$. ν = 50 mV s^{-1}.

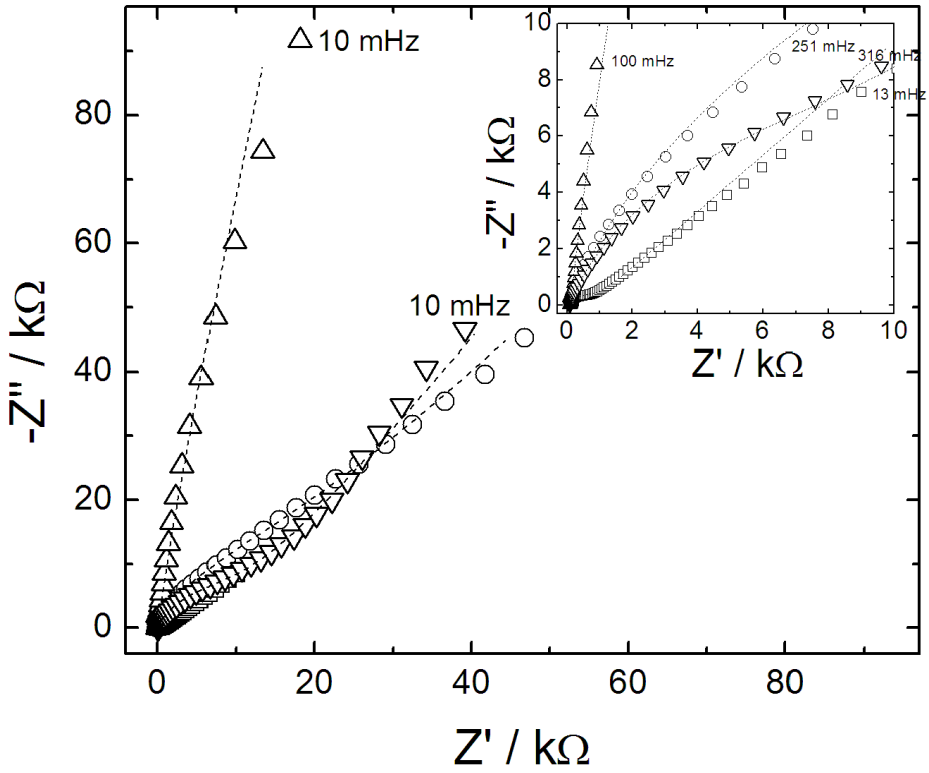

Figure S19. Impedance plane plots for bare GC (⭘) and, after 30 HCV scans in 0.1 M KH_2PO_4 (pH 6.5) containing 100 mM ethanol, for GC/VC XC-72/PM/Nafion (ᔓ), GC/VC XC-72/PM-ADH/Nafion (❒), and GC/VC XC-72/PM-ADH-NAD^+/Nafion (♦) electrodes in N_2-saturated 0.1 M KH_2PO_4 (pH 6.5) containing 1 m$MK_3Fe(CN)_6$. Potential perturbation: 25 mV (rms). Frequency range: 100 kHz–10 mHz. Constant potential for EIS acquisition: OCP (0.26 V *vs*. SCE on average). Lines represent spectra (adjusted) calculated using a non-linear least-squares program, conforming to the equivalent circuit $R_s[Q_{dl}(R_{ct}W_{lf})]$, or $R_s[Q_{dl}(R_{ct}Q_{lf})]$. Calculated average values: R_s = 83 Ω, Q_{dl} = 22 μF s^{n-1}, n = 0.8, and W_{lf} = 122 μF. Inset: Impedance plane plots from the main graph restricted to 10 kΩ.

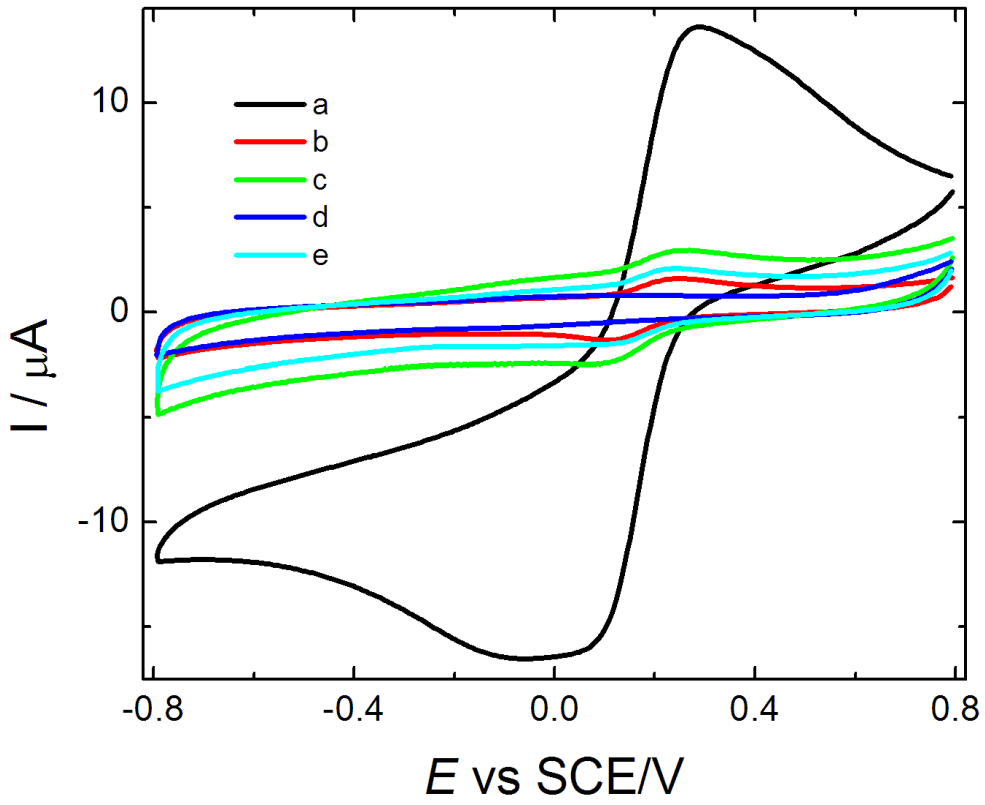

Figure S20. Cyclic voltammograms after 5 HCV scans in 0.1 M KH_2PO_4 (pH 6.5) containing 100 mM ethanol for bare GC at 20 mV s^{-1} (*a*), and GC/PM-ADH-NAD^+/Nafion electrodes at 20 (*b*), 50 (*c*), 80 (*d*), and 120 mV s^{-1} (*e*) in N_2-saturated 0.1 M KH_2PO_4 (pH 6.5) containing 1 mM $K_3Fe(CN)_6$. ν = 50 mV s^{-1}.

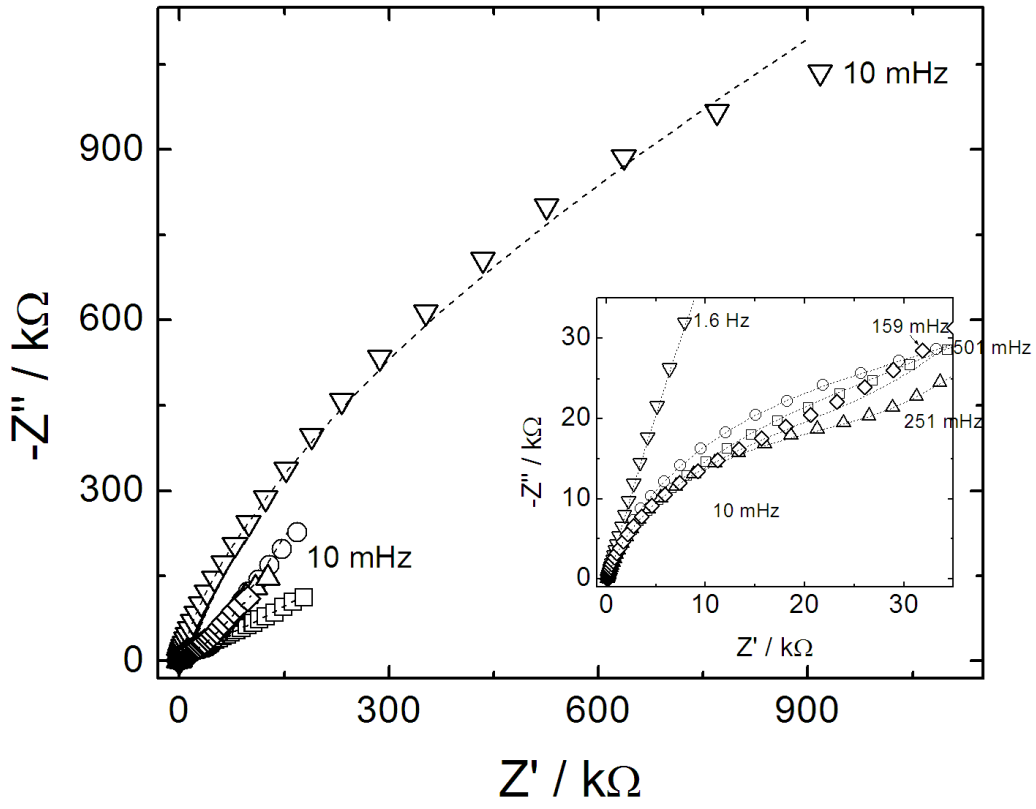

Figure S21. Impedance plane plots after 5 HCV scans in 0.1 M KH_2PO_4 (pH 6.5) containing 100 mM ethanol for bare GC at 20 mV s^{-1} (⭘) and GC/PM-ADH-NAD^+/Nafion electrodes at 20 (ᔓ), 50 (❒), 80 (♦), and 120 mV s^{-1} (✵) in N_2-saturated 0.1 M KH_2PO_4 (pH 6.5) containing 1 m$MK_3Fe(CN)_6$. Potential perturbation: 25 mV (rms). Frequency range: 100 kHz–10 mHz. Constant potential for EIS acquisition: OCP (0.20 V *vs*. SCE on average). Lines represent spectra (adjusted) calculated using a non-linear least-squares program, conforming to the equivalent circuit $R_s[Q_{dl}(R_{ct}W_{lf})]$, or $R_s[Q_{dl}(R_{ct}Q_{lf})]$. Calculated average values: R_s = 86 Ω, Q_{dl} = 6 μF s^{n-1}, n = 0.9, and W_{lf} = 80 μF. Inset: Impedance plane plots from the main graph restricted to 35 kΩ.

Table S1. Approximate R_{ct} and k^0 (or $k_{app}{}^0$) values obtained from non-linear least-squares calculations for elements of the equivalent circuit $R_s[Q_{dl}(R_{ct}W_{lf})]$, or $R_s[Q_{dl}(R_{ct}Q_{lf})]$, adjusted for EIS responses (Figures S11, S13, S15, S17, and S19) provided by bare GC, GC/NAD$^+$/Nafion, GC/NADH/Nafion, GC/VC XC-72/PM/Nafion, GC/VC XC-72/PM-ADH/Nafion, GC/ADH-NAD$^+$/Nafion, GC/ADH-NADH/Nafion, GC/PM-ADH-NAD$^+$/Nafion, GC/PM-ADH-NADH/Nafion, and GC/VC XC-72/PM-ADH-NAD$^+$/Nafion electrodes in N_2-saturated 0.1 M KH_2PO_4 (pH 6.5) containing 1 mM $K_3Fe(CN)_6$.

Electrode	R_{ct} (kΩ)	k^0 or $k_{app}{}^0$ (cm s^{-1} × 10^5)[a]
Bare GC	0.75	180
GC/NAD$^+$/Nafion after 30 HCV scans in 0.1 M KH_2PO_4 (pH 6.5) (Figure S11)	5	28
GC/NADH/Nafion after 30 HCV scans in 0.1 M KH_2PO_4 (pH 6.5) (Figure S11)	14	10
GC/ADH-NAD$^+$/Nafion after 30 HCV scans in 0.1 M KH_2PO_4 (pH 6.5) (Figure S13)	433	0.3
GC/ADH-NADH/Nafion after 30 HCV scans in 0.1 M KH_2PO_4 (pH 6.5) (Figure S13)	232	0.6
GC/PM-ADH-NAD$^+$/Nafion after 30 HCV scans in 0.1 M KH_2PO_4 (pH 6.5) (Figure S13)	74	1.8
GC/VC XC-72/PM-ADH/Nafion after 30 HCV scans in 0.1 M KH_2PO_4 (pH 6.5) (Figure S13)	10	14
GC/NAD$^+$/Nafion after 30 HCV scans in 0.1 M KH_2PO_4 (pH 6.5) containing 100 mM ethanol (Figure S15)	20	6.6
GC/NAD$^+$/Nafion' after 30 HCV scans in 0.1 M KH_2PO_4 (pH 6.5) containing 100 mM ethanol (Figure S15)	4.2	32
GC/NADH/Nafion after 30 HCV scans in 0.1 M KH_2PO_4 (pH 6.5) containing 100 mM ethanol (Figure S15)	12	11
GC/ADH-NAD$^+$/Nafion after 30 HCV scans in 0.1 M KH_2PO_4 (pH 6.5) containing 100 mM ethanol (Figure S15)	51	2.6
GC/ADH-NADH/Nafion after 30 HCV scans in 0.1 M KH_2PO_4 (pH 6.5) containing 100 mM ethanol (Figure S15)	132	1.0
GC/ADH-NAD$^+$/Nafion after 30 HCV scans in 0.1 M KH_2PO_4 (pH 6.5) containing 100 mM ethanol (Figure S17)	2161	0.06
GC/ADH-NAD$^+$/Nafion after 30 HCV scans in 0.1 M KH_2PO_4 (pH 6.5) containing 100 mM ethanol (narrow potential scan window) (Figure S17)	193	0.7
GC/PM-ADH-NAD$^+$/Nafion after 30 HCV	212	0.6

scans in 0.1 M KH_2PO_4 (pH 6.5) containing 100 mM ethanol (Figure S17)		
GC/ADH-NADH/Nafion after 30 HCV scans in 0.1 M KH_2PO_4 (pH 6.5) containing 100 mM ethanol (Figure S17)	103	1.3
GC/PM-ADH-NADH/Nafion after 30 HCV scans in 0.1 M KH_2PO_4 (pH 6.5) containing 100 mM ethanol (Figure S17)	31	4.2
GC/VC XC-72/PM/Nafion after 30 HCV scans in 0.1 M KH_2PO_4 (pH 6.5) containing 100 mM ethanol (Figure S19)	24	5.6
GC/VC XC-72/PM-ADH-NAD^+/Nafion after 30 HCV scans in 0.1 M KH_2PO_4 (pH 6.5) containing 100 mM ethanol (Figure S19)	14	9.3

[a] k^0 (or k_{app}^0) values were obtained from R_{ct} as described in references [1-4].

Table S2. Approximate R_{ct} and k^0 (or k_{app}^0) values obtained from non-linear least-squares calculations for elements of the equivalent circuit $R_s[Q_{dl}(R_{ct}W_{lf})]$, or $R_s[Q_{dl}(R_{ct}Q_{lf})]$, adjusted for EIS responses (Figure S21) provided by bare GC and GC/PM-ADH-NAD^+/Nafion electrodes in N_2-saturated 0.1 M KH_2PO_4 (pH 6.5) containing 1 mM $K_3Fe(CN)_6$, after five HCV scansin N_2-saturated 0.1 M KH_2PO_4 (pH 6.5) containing 100 mM ethanol.

Electrode	R_{ct} (kΩ)	k^0 or k_{app}^0 (cm $s^{-1} \times 10^5$)[a]
Bare GC (20 mV s^{-1})	23	5.7
GC/PM-ADH-NAD^+/Nafion (20 mV s^{-1})	54	2.5
GC/PM-ADH-NAD^+/Nafion (50 mV s^{-1})	36	3.7
GC/PM-ADH-NAD^+/Nafion (80 mV s^{-1})	874	0.2
GC/PM-ADH-NAD^+/Nafion (120 mV s^{-1})	33	4.0

[a] k^0 (or k_{app}^0) values were obtained from R_{ct} as described in references [1-4].

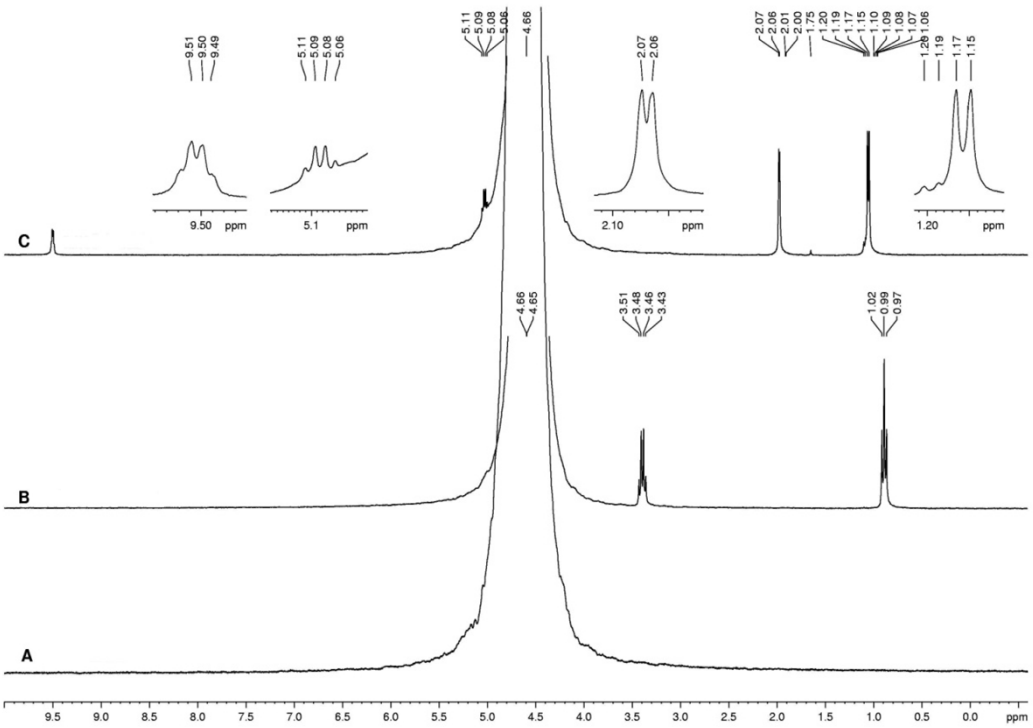

Figure S22. ^{1}H NMR spectrum for aliquots of 0.1 M KH_2PO_4 (pH 6.5) (A), 0.1 M KH_2PO_4 (pH 6.5) containing 100 mM ethanol (B), and 0.1 M KH_2PO_4 (pH 6.5) containing 20 mM acetaldehyde (C). Insets depict the range comprising the hydrogen in acetaldehyde and the hydrated form of acetaldehyde.

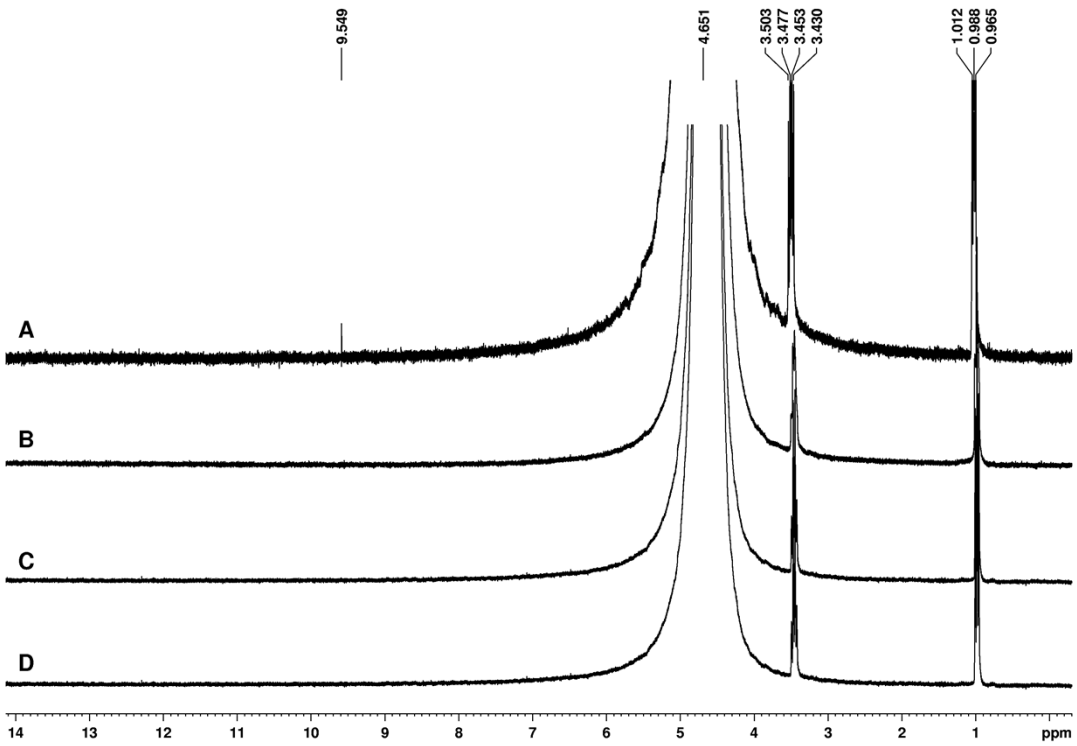

Figure S23. ^{1}H NMR spectra for aliquots of 0.1 M KH_2PO_4 (pH 6.5) containing 100 mM ethanol (A) after the GC/PM-ADH-NAD^+/Nafion electrode was subjected to ω = 200 rpm for 3 h followed by 5 HCV scans, (B) after the GC/ADH/Nafion electrode underwent 30 HCV scans, (C) after the GC/PM-ADH/Nafion electrode underwent 30 HCV scans, and (D) after the GC/PM-ADH-NAD^+/Nafion electrode underwent 3 hours under ω = 200 rpm.

REFERENCES

[1] S. R. Santos and G. Maia, *Electrochim. Acta* 2012, **71**, 116–122.
[2] A. H. H. Tanji, F. Lima, S. R. Santos and G. Maia, *J. Phys. Chem. C* 2012, **116**, 18857–18864.
[3] L. B. Venarusso, K. Tammeveski and G. Maia, *Electrochim. Acta* 2011, **56**, 8926–8933.
[4] F. Lima, G. V. Fortunato and G. Maia, *RSC Advances* 2013, **3**, 9550–9560.